

Soft end-point and mass corrections to the $\eta'g^*g^*$ vertex function

S.S. Agaev^{1,a}, M.A. Gomshi Nobary^{2,b}

¹ Institute for Physical Problems, Baku State University, Z. Khalilov st. 23, 1148 Baku, Azerbaijan

² Department of Physics, Faculty of Science, Razi University, Kermanshah, Iran

Received: 25 June 2007 / Revised version: 5 November 2007 /

Published online: 1 February 2008 – © Springer-Verlag / Società Italiana di Fisica 2008

Abstract. Power-suppressed corrections arising from end-point integration regions to the space-like vertex function of the massive η' -meson virtual gluon transition $\eta' - g^*g^*$ are computed. Calculations are performed within the standard hard-scattering approach (HSA) and the running coupling method supplemented by the infrared renormalon calculus. Contributions to the vertex function from the quark and gluon contents of the η' -meson are taken into account and the Borel resummed expressions for $F_{\eta'g^*g^*}(Q^2, \omega, \eta)$, as well as for $F_{\eta'gg^*}(Q^2, \omega = \pm 1, \eta)$ and $F_{\eta'g^*g^*}(Q^2, \omega = 0, \eta)$ are obtained. It is demonstrated that the power-suppressed corrections $\sim (\Lambda^2/Q^2)^n$, in the explored range of the total gluon virtuality $1 \leq Q^2 \leq 25 \text{ GeV}^2$, considerably enhance the vertex function relative to the results found in the framework of the standard HSA with a fixed coupling. Modifications generated by the η' -meson mass effects are discussed.

PACS. 12.38.Bx; 14.40.Aq; 11.10.Hi

1 Introduction

Recently interest in theoretical investigations of the gluonic structure of the η and η' -mesons has risen due to the high precision CLEO results on the electromagnetic $\eta\gamma$, $\eta'\gamma$ transition form factors (FFs) [1], as well as because of the observed large branching ratios for the exclusive $B \rightarrow K + \eta'$ and semi-inclusive $B \rightarrow \eta' + X_s$ decays [2, 3].

The data on FF of the $\eta'\gamma$ transition were mainly used for extracting constraints on the quark component of the η' -meson distribution amplitude (DA) [4–6]. In these investigations various theoretical schemes and methods were employed. An important conclusion drawn from these studies is that the quark component of the η' -meson DA should be close to its asymptotic form and that the admixture of the first non-asymptotic term should be within the range of $B_2^q(1 \text{ GeV}^2) \simeq 0.05\text{--}0.15$, B_2^q being the first Gegenbauer coefficient.

An effect of the gluon component of the η' -meson DA on the $\eta'\gamma$ transition was analyzed in [7, 8], where relevant constraints on the input parameters B_2^q and B_2^g were extracted: it was shown that their allowed values are strongly correlated. Useful bounds on the Gegenbauer coefficients B_2^q and B_2^g were obtained also from investigation of the semi-inclusive decay $\Upsilon(1S) \rightarrow \eta' + X$ [9].

The two-gluon valence Fock component of the η' -meson can directly contribute to the $\eta'\gamma$ transition FF only at the next-to-leading order due to quark box diagrams and also affect the leading order result through evolution of the quark component of the η' -meson DA. Hence, an effect of the η' -meson gluon component on the $\eta'\gamma$ transition is mild. Contrary, the contribution of the gluon content of the η' -meson to the two-body non-leptonic exclusive and semi-inclusive decay ratios of the B -meson may be sizeable. Indeed, in order to explain the observed large branching ratio $\text{Br}(B \rightarrow \eta' + X_s)$, in [10] a mechanism that employs the two-gluon content of the η' -meson was suggested. In accordance with this approach the dominant fraction of the $B \rightarrow \eta' + X_s$ decay rate appears as the result of the transition $g^* \rightarrow g\eta'$ of a virtual gluon from the standard model penguin diagram $b \rightarrow sg^*$. In [10] the g^*gn' vertex function (VF) was approximated by the constant $H(q^2, 0, m_{\eta'}^2) \simeq H(0, 0, m_{\eta'}^2) \simeq 1.8 \text{ GeV}^{-1}$, the latter being extracted from the analysis of the $J/\psi \rightarrow \eta'\gamma$ decay. Further investigations demonstrated that the effects of the QCD running coupling $\alpha_s(q^2)$ [11], as well as the momentum dependence of the form factor $H(q^2, 0, m_{\eta'}^2)$, properly taken into account, considerably reduce the contribution to $\text{Br}(B \rightarrow \eta' + X_s)$ of the mechanism under consideration [12]. To eliminate the discrepancy between theoretical predictions and the experimental data in [13] a gluon fusion mechanism was proposed. In accordance with the latter, the η' -meson is

^a e-mail: agaev_shahin@yahoo.com

^b e-mail: mnobary@razi.ac.ir

produced by the fusion of a gluon from the QCD penguin diagram $b \rightarrow sg^*$ with another one emitted by the light quark inside the B -meson. In this mechanism, the vertex function $F_{\eta'g^*g^*}(q_1^2, q_2^2, m_{\eta'}^2)$ appears owing to the $g^*g^* \rightarrow \eta'$ transition. Similar ideas form a basis for the computation of the branching ratios of various two-body non-leptonic exclusive decay modes and transition FFs of the B meson [14–20].

Hence, the η' -meson virtual (on-shell) gluon transition VF, $F_{\eta'g^*g^*}(q_1^2, q_2^2, m_{\eta'}^2)$, is the central ingredient of the relevant analysis performed within perturbative QCD (pQCD) and it deserves further investigations. This VF was computed in numerous works [8, 21–23]. The space-like massless $\eta'g^*g^*$ vertex within the standard hard-scattering approach (HSA) was considered in [8], where a correct analysis of the normalization of the gluon component of the η' -meson DA and that of the gluon projector onto a pseudo-scalar meson state was performed. Power-suppressed corrections, arising from the end-point integration regions $x \rightarrow 0, 1$, to the massless space-like $\eta'g^*g^*$ VF were found in [22]. In this work the standard HSA and the running coupling (RC) method together with the infrared (IR) renormalon calculus were applied. The η' -meson mass corrections to the $\eta'g^*g^*$ space- and time-like vertex in the standard HSA were calculated in [23].

In the present work, we extend the results obtained in [22] by taking into account the η' -meson mass effects, which may be considerable. The RC method [24, 25] enables us to estimate power corrections coming from the end-point $x \rightarrow 0, 1$ regions in the integrals determining the amplitude of the $\eta'g^*g^*$ transition. Indeed, in the framework of the standard HSA [26–28], in order to calculate the amplitude of the process, one has to perform integrations over the longitudinal momentum fractions of the constituents of the meson. If one chooses the renormalization scale μ_R^2 in the hard-scattering amplitude T_H of the corresponding partonic subprocess in such a way as to minimize higher-order corrections and allows the QCD coupling constant α_s (μ_R^2) to run, then one encounters divergences arising from the end-point $x \rightarrow 0, 1$ regions. The reason is that the scale μ_R^2 , as a rule, is equal to the momentum squared of the hard virtual partons carrying the strong interactions in the subprocess' Feynman diagrams and depends, in general, on x (or $\bar{x} \equiv 1 - x$). Within the RC method this problem is resolved by applying the renormalization group equation and the IR renormalon calculus (for a review see, [29, 30]). It turns out that such a treatment allows us to evaluate power corrections to the physical quantity under consideration [6, 7, 22, 31–33].

This paper is structured as follows. In Sect. 2 we present the necessary information on the quark–gluon structure of the η' -meson, its DAs and the hard-scattering amplitudes of the relevant subprocesses. Section 3 is devoted to a calculation of the quark component of the $\eta'g^*g^*$ vertex function. The contribution to the VF of the gluon content of the η' -meson is computed in Sect. 4. Section 5 contains our numerical results and their analysis. In Sect. 6 we make our concluding remarks.

2 Quark and gluon content of the η' -meson and the $\eta'g^*g^*$ vertex

The Fock state decomposition of the pseudoscalar $P = \eta, \eta'$ -mesons can be written in the following form:

$$|P\rangle = |P_a\rangle + |P_b\rangle + |P_c\rangle + |P_g\rangle ,$$

where $|P_a\rangle$ and $|P_b\rangle$ denote the P -meson light quarks, and $|P_c\rangle$ and $|P_g\rangle$ its charm and gluon components, respectively.

The light-quark content of the P -meson can be described either in the $SU_f(3)$ octet–singlet or in the quark-flavor basis. In this paper we choose to work in the quark-flavor basis

$$|\eta_q\rangle = \frac{\Psi_q}{\sqrt{2}} |u\bar{u} + d\bar{d}\rangle , \quad |\eta_s\rangle = \Psi_s |\bar{s}\rangle . \quad (1)$$

Here Ψ_i denote wave functions of the corresponding parton states.

We neglect the charm component of the η' -meson, because in accordance with existing estimations [34–36], it is too small to affect considerably the B -meson exclusive decays.

The pure light-quark sector of the $\eta-\eta'$ system without charm and gluon admixtures can be treated as superpositions of the basic states (1),

$$|\eta\rangle = \cos \phi_p |\eta_q\rangle - \sin \phi_p |\eta_s\rangle , \\ |\eta'\rangle = \sin \phi_p |\eta_q\rangle + \cos \phi_p |\eta_s\rangle . \quad (2)$$

One of the advantages of the quark-flavor basis is that in this basis the decay constants $f_P^{q(s)}$ follow with great accuracy the pattern of the state mixing [37]

$$f_\eta^q = f_q \cos \phi_p, \quad f_\eta^s = -f_s \sin \phi_p , \\ f_{\eta'}^q = f_q \sin \phi_p, \quad f_{\eta'}^s = f_s \cos \phi_p , \quad (3)$$

where the decay constants f_q and f_s and the mixing angle ϕ_p have the values

$$f_q = (1.07 \pm 0.02) f_\pi, \quad f_s = (1.34 \pm 0.06) f_\pi , \\ \phi_p = 39.3^\circ \pm 1.0^\circ , \quad (4)$$

with $f_\pi = 0.131$ GeV being the pion weak decay constant.

The singlet part of the η' -meson DA, which is only relevant to our present investigations, depends on both the quark $\phi^q(x, \mu^2)$ and gluon $\phi^g(x, \mu^2)$ components of the η' -meson DA. These functions satisfy the symmetry and antisymmetry conditions under the exchange $x \leftrightarrow \bar{x}$,

$$\phi^q(x, \mu^2) = \phi^q(\bar{x}, \mu^2), \quad \phi^g(x, \mu^2) = -\phi^g(\bar{x}, \mu^2) , \quad (5)$$

and they are given by the expressions

$$\phi^q(x, \mu_F^2) = 6Cx\bar{x} \left\{ 1 + \sum_{n=2,4,\dots}^{\infty} \left[B_n^q \left(\frac{\alpha_s(\mu_0^2)}{\alpha_s(\mu_F^2)} \right)^{\frac{\gamma_+^n}{\beta_0}} \right. \right. \\ \left. \left. + \rho_n^g B_n^g \left(\frac{\alpha_s(\mu_0^2)}{\alpha_s(\mu_F^2)} \right)^{\frac{\gamma_-^n}{\beta_0}} \right] C_n^{3/2}(x - \bar{x}) \right\} \quad (6)$$

and

$$\phi^g(x, \mu_F^2) = Cx\bar{x} \sum_{n=2,4..}^{\infty} \left[\rho_n^q B_n^q \left(\frac{\alpha_s(\mu_0^2)}{\alpha_s(\mu_F^2)} \right)^{\frac{\gamma_n^q}{\beta_0}} + B_n^g \left(\frac{\alpha_s(\mu_0^2)}{\alpha_s(\mu_F^2)} \right)^{\frac{\gamma_n^g}{\beta_0}} \right] C_{n-1}^{5/2}(x - \bar{x}), \quad (7)$$

where the constant C is defined as

$$C = \sqrt{2} f_q \sin \phi_p + f_s \cos \phi_p.$$

In (6) and (7), $C_n^{3/2}(z)$ and $C_{n-1}^{5/2}(z)$ are Gegenbauer polynomials, μ_F^2 and μ_0^2 are the factorization and normalization scales, respectively. The values of the input parameters B_n^q and B_n^g have to be fixed at the normalization scale $\mu_0^2 = 1 \text{ GeV}^2$: they determine the shape of the DAs. In the above expressions, $\alpha_s(\mu^2)$ is the QCD coupling constant in the two-loop approximation given by

$$\alpha_s(\mu^2) = \frac{4\pi}{\beta_0 \ln(\mu^2/\Lambda^2)} \left[1 - \frac{2\beta_1}{\beta_0^2} \frac{\ln \ln(\mu^2/\Lambda^2)}{\ln(\mu^2/\Lambda^2)} \right], \quad (8)$$

with β_0 and β_1 being the one- and two-loop coefficients of the QCD beta function

$$\beta_0 = 11 - \frac{2}{3} n_f, \quad \beta_1 = 51 - \frac{19}{3} n_f. \quad (9)$$

Here, Λ is the QCD scale parameter and n_f is number of active quark flavors.

In this work, we shall use the η' -meson DA that contains only the first non-asymptotic terms. Stated differently, we suppose that in (6) and (7) $B_2^q \neq 0$, $B_2^g \neq 0$ and $B_n^q = B_n^g = 0$ for all $n \geq 4$. Taking into account the expressions for the required Gegenbauer polynomials as well as the values of the relevant parameters, we can recast the η' -meson quark and gluon DAs into the following simple forms [22]:

$$\begin{aligned} \phi^q(x, \mu_F^2) &= 6Cx\bar{x} [1 + A(\mu_F^2) - 5A(\mu_F^2)x\bar{x}], \\ \phi^g(x, \mu_F^2) &= Cx\bar{x}(x - \bar{x})B(\mu_F^2). \end{aligned} \quad (10)$$

For $n_f = 4$ the functions $A(\mu_F^2)$ and $B(\mu_F^2)$ are defined by

$$\begin{aligned} A(\mu_F^2) &= 6B_2^q \left(\frac{\alpha_s(\mu_F^2)}{\alpha_s(\mu_0^2)} \right)^{\frac{48}{75}} - \frac{B_2^g}{17} \left(\frac{\alpha_s(\mu_F^2)}{\alpha_s(\mu_0^2)} \right)^{\frac{107}{75}}, \\ B(\mu_F^2) &= 19B_2^q \left(\frac{\alpha_s(\mu_F^2)}{\alpha_s(\mu_0^2)} \right)^{\frac{48}{75}} + 5B_2^g \left(\frac{\alpha_s(\mu_F^2)}{\alpha_s(\mu_0^2)} \right)^{\frac{107}{75}}. \end{aligned} \quad (11)$$

The η' -meson quark and gluon DAs for $n_f = 3$ can be found in [22].

The η' -meson virtual gluon transition vertex function $F_{\eta' g^* g^*}(Q^2, \omega, \eta)$ is the sum of the quark and gluon components defined in terms of the invariant amplitudes for the

process

$$\eta'(P) \rightarrow g^*(q_1) + g^*(q_2),$$

in the following way:

$$M^{q(g)} = -iF_{\eta' g^* g^*}^{q(g)}(Q^2, \omega, \eta) \delta_{ab} \epsilon^{\mu\nu\rho\sigma} \epsilon_\mu^{a*} \epsilon_\nu^{b*} q_1 \rho q_2 \sigma. \quad (12)$$

Here, ϵ_μ^a , ϵ_ν^b and q_1 , q_2 are the polarization vectors and four-momenta of the two gluons, respectively. Because we study only the space-like VF, q_1^2 and q_2^2 obey the constraints $Q_1^2 = -q_1^2 \geq 0$ and $Q_2^2 = -q_2^2 \geq 0$. The VF, $F_{\eta' g^* g^*}(Q^2, \omega, \eta)$, depends on the total gluon virtuality Q^2 , the asymmetry parameter ω , and η' -meson scaled mass η

$$Q^2 = Q_1^2 + Q_2^2, \quad \omega = \frac{Q_1^2 - Q_2^2}{Q^2}, \quad \eta = \frac{m_{\eta'}^2}{Q^2}. \quad (13)$$

The parameter ω varies in the region $-1 \leq \omega \leq 1$. The values $\omega = \pm 1$ corresponds to the η' -meson on-shell gluon transition and $\omega = 0$ to the situation when the gluons have equal virtualities.

In accordance with the factorization theorems of pQCD, at high momentum transfer the components of the VF $F_{\eta' g^* g^*}^{q(g)}(Q^2, \omega, \eta)$ can be calculated by means of the formulas

$$\begin{aligned} F_{\eta' g^* g^*}^q(Q^2, \omega, \eta) &= \int_0^1 [T_1^q(x, Q^2, \omega, \eta, \mu_F^2) \\ &\quad + T_2^q(x, Q^2, \omega, \eta, \mu_F^2)] \phi^q(x, \mu_F^2) dx, \end{aligned} \quad (14)$$

and

$$\begin{aligned} F_{\eta' g^* g^*}^g(Q^2, \omega, \eta) &= \int_0^1 [T_1^g(x, Q^2, \omega, \eta, \mu_F^2) \\ &\quad - T_2^g(x, Q^2, \omega, \eta, \mu_F^2)] \phi^g(x, \mu_F^2) dx. \end{aligned} \quad (15)$$

The sum

$$\begin{aligned} T_H^q(x, Q^2, \omega, \eta, \mu_F^2) &= T_1^q(x, Q^2, \omega, \eta, \mu_F^2) \\ &\quad + T_2^q(x, Q^2, \omega, \eta, \mu_F^2) \end{aligned}$$

and the difference

$$\begin{aligned} T_H^g(x, Q^2, \omega, \eta, \mu_F^2) &= T_1^g(x, Q^2, \omega, \eta, \mu_F^2) \\ &\quad - T_2^g(x, Q^2, \omega, \eta, \mu_F^2) \end{aligned}$$

are the hard-scattering amplitudes of the subprocesses $q + \bar{q} \rightarrow g^* + g^*$ and $g + g \rightarrow g^* + g^*$, respectively. The Feynman diagrams contributing at the leading order to these subprocesses are depicted in Figs. 1 and 2.

At the leading order of pQCD, the hard-scattering amplitudes do not depend on the factorization scale μ_F^2 but depend implicitly on the renormalization scale μ_R^2 through $\alpha_s(\mu_R^2)$. As the scales μ_R^2 and μ_F^2 are independent of each other and can be chosen separately, we adopt in this work the standard choice for the factorization scale $\mu_F^2 = Q^2$,

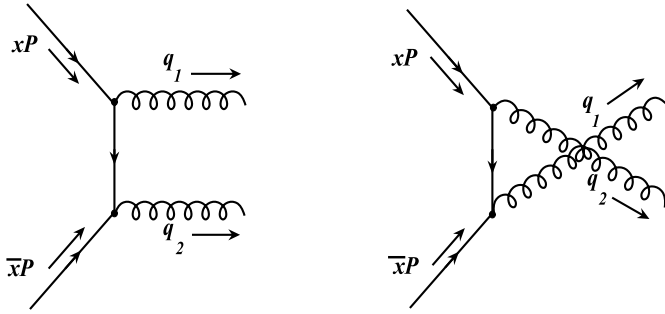


Fig. 1. Leading-order Feynman diagrams contributing to the hard-scattering subprocess $q + \bar{q} \rightarrow g^* + g^*$

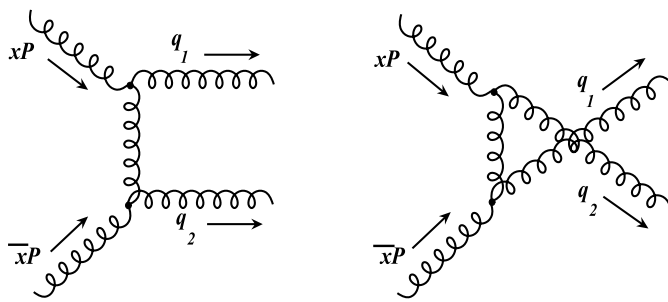


Fig. 2. Feynman diagrams contributing at leading order to the subprocess $g + \bar{g} \rightarrow g^* + g^*$

and we omit in what follows the dependence of the hard-scattering amplitudes on μ_F^2 . Thus, we have

$$T_1^g(x, Q^2, \omega, \eta, \mu_R^2) = -\frac{2\pi}{3Q^2} \frac{\alpha_s(\mu_R^2)}{\omega\lambda} \times \frac{\omega(1+\lambda) - \eta(x-\bar{x})}{x(1+\omega) + \bar{x}(1-\omega) + 2x\bar{x}\eta} \quad (16)$$

and

$$T_1^g(x, Q^2, \omega, \eta, \mu_R^2) = \frac{\pi\alpha_s(\mu_R^2)}{Q^2 n_f} \times \frac{x(1+\omega) + \bar{x}(1-\omega) + 2(1+x\bar{x})\eta}{\omega\lambda [\bar{x}(1+\omega) + x(1-\omega) + 2x\bar{x}\eta]}, \quad (17)$$

where $\lambda = (1 + 2\eta/\omega^2 + \eta^2/\omega^2)^{1/2}$ [23]. The remaining two functions can be obtained from (16) and (17) by means of the replacement $x \leftrightarrow \bar{x}$.

In the standard HSA one sets the renormalization scale to be $\mu_R^2 = Q^2$, fixing $\alpha_s(\mu_R^2)$ with respect to x , and simplifying the calculation of the VF considerably. In this approach the functions (16) and (17) possess the symmetry features

$$T_{1(2)}^g(x, Q^2, -\omega, \eta) = T_{2(1)}^g(x, Q^2, \omega, \eta), \\ T_{1(2)}^g(x, Q^2, -\omega, \eta) = -T_{2(1)}^g(x, Q^2, \omega, \eta). \quad (18)$$

Using these features as well as (5) and the symmetry properties of $T_{1(2)}^{q(g)}$ under $x \leftrightarrow \bar{x}$ exchange, one can prove that

$$F_{\eta' g^* g^*}^{q(g)}(Q^2, \omega, \eta) = F_{\eta' g^* g^*}^{q(g)}(Q^2, -\omega, \eta). \quad (19)$$

The last equality is a manifestation of the Bose symmetry of the process under discussion under vector particles–gluons exchange.

Within the RC method the renormalization scale μ_R^2 is chosen equal, as a rule, to the momentum squared $|q^2|$ of the virtual partons in the corresponding Feynman diagrams. For the massless η' -meson on-shell gluon transition the scale μ_R^2 is exactly equal to

$$\mu_R^2 = Q^2 x. \quad (20)$$

Then upon $x \leftrightarrow \bar{x}$ exchange, the argument of $\alpha_s(\bar{x})$ in the functions $T_2^{q(g)}$ becomes equal to $\bar{x} = Q^2 \bar{x}$. In the general case, the absolute value of the square of the four-momenta q^2 of the virtual partons depends on the total gluon virtuality Q^2 , the asymmetry parameter ω and the scaled mass term η . However, to avoid problems related to the appearance of the parameters Q^2 , ω and η in the argument of α_s , we shall use the renormalization scale (20). Such a choice is justified from the physics point of view as well, because namely the part $\sim Q^2 x$ of the renormalization scale leads to the power corrections $\sim (\Lambda^2/Q^2)^n$, $n = 1, 2, \dots$ to the VF $F_{\eta' g^* g^*}(Q^2, \omega, \eta)$, which we are going to compute.

In the present paper we adopt the symmetrized RC method, where $\alpha_s(Q^2 x)$ and $\alpha_s(Q^2 \bar{x})$ are replaced by

$$\frac{\alpha_s(Q^2 x) + \alpha_s(Q^2 \bar{x})}{2}.$$

After this modification all symmetry properties of the hard-scattering amplitudes and the vertex function remain valid within the RC method as well. The symmetrized RC method was successfully employed in the investigation of various exclusive processes [22, 32, 33].

3 Quark component of the vertex function

$$F_{\eta' g^* g^*}^q(Q^2, \omega, \eta)$$

The expression for the quark component of the vertex function $F_{\eta' g^* g^*}^q(Q^2, \omega, \eta)$ can be computed only after resolving the problems of the soft end-point regions $x \rightarrow 0, 1$. In fact, having inserted the explicit expressions of the hard-scattering amplitude and the quark component of the η' -meson DA into (14), one encounters divergences arising from the singularities of the coupling constants $\alpha_s(Q^2 x)$ and $\alpha_s(Q^2 \bar{x})$ in the limits $x \rightarrow 0, 1$. The RC method provides the required prescription to cure these divergences.

To this end, we express the running coupling $\alpha_s(Q^2 x)$ in terms of $\alpha_s(Q^2)$ and, as a result, obtain integrals that can be regularized and calculated using the approach described in [24, 25]. Then the quark component of the VF is written as a perturbative series in $\alpha_s(Q^2)$ with factorially growing coefficients. The resummation of such a series

is performed by means of a Borel transformation. Namely, one has to determine the Borel transform of the corresponding series and in order to get the resummed expression for the vertex function one has to invert the Borel transform. The Borel transform of the series with factorially growing coefficients contains infrared renormalon poles located at the positive axis of the Borel plane; therefore the inverse Borel transformation suffers from pole divergences. In other words, the Borel technique transforms the endpoint divergences into the IR renormalon pole divergences of the inverse transformation. Then, the resummed expression can be extracted by computing the relevant integrals in the sense of the Cauchy principal value [29, 30].

A useful way to bypass these intermediate operations and directly obtain the Borel resummed expressions is to introduce the following formula for $\alpha_s(Q^2 x)$ [6]:

$$\alpha_s(Q^2 x) = \frac{4\pi}{\beta_0} \int_0^\infty du \exp(-ut) R(u, t) x^{-u}, \quad (21)$$

where the function $R(u, t)$ is defined as

$$R(u, t) = 1 - \frac{2\beta_1}{\beta_0^2} u (1 - \gamma - \ln t - \ln u).$$

In the above, $\gamma \simeq 0.577216$ is the Euler constant and $t = \ln(Q^2/\Lambda^2)$.

Calculations of the quark component of the VF lead to the following result:

$$F_{\eta' g^* g^*}^q(Q^2, \omega, \eta) = F_1^q(Q^2, \omega, \eta) + F_2^q(Q^2, \omega, \eta), \quad (22)$$

where

$$\begin{aligned} F_i^q(Q^2, \omega, \eta) &= -\frac{16\pi^2 C[1+A(Q^2)]}{Q^2 \beta_0} K_i(\omega, \eta) \\ &\times \int_0^\infty du e^{-ut} R(u, t) B(2-u, 2) \\ &\times [2F_1(1, 2; 4-u; r_i) + 2F_1(1, 2-u; 4-u; r_i)] \\ &+ \frac{80\pi^2 C A(Q^2)}{Q^2 \beta_0} K_i(\omega, \eta) \\ &\times \int_0^\infty du e^{-ut} R(u, t) B(3-u, 3) \\ &\times [2F_1(1, 3; 6-u; r_i) + 2F_1(1, 3-u; 6-u; r_i)]. \end{aligned} \quad (23)$$

Here

$$K_1(\omega, \eta) = \frac{\eta}{\omega\lambda(\omega\lambda - \omega - \eta)}, \quad r_1 = \frac{2\eta}{\omega + \eta - \omega\lambda} \quad (24)$$

and

$$K_2(\omega, \eta) = \frac{\eta}{\omega\lambda(\omega\lambda - \omega + \eta)}, \quad r_2 = \frac{2\eta}{\eta - \omega + \omega\lambda}. \quad (25)$$

Equation (22) with the functions F_1^q and F_2^q is the Borel resummed expression for the quark component of the $\eta' g^* g^*$

vertex function and contains power-suppressed corrections coming from the soft end-point regions [22].

Since under the replacement $\omega \leftrightarrow -\omega$ the relations $K_1 \leftrightarrow K_2$ and $r_1 \leftrightarrow r_2$ hold, we get

$$F_{\eta' g^* g^*}^q(Q^2, -\omega, \eta) = F_{\eta' g^* g^*}^q(Q^2, \omega, \eta).$$

The components $F_1^q(Q^2, \omega, \eta)$ and $F_2^q(Q^2, \omega, \eta)$ of $F_{\eta' g^* g^*}^q(Q^2, \omega, \eta)$ can be obtained from each other utilizing the transformation

$${}_2F_1(a, b; c; z) = (1-z)^{-a} {}_2F_1\left(a, c-b; c; \frac{z}{z-1}\right). \quad (26)$$

The argument r_1 of the hypergeometric functions in $F_1^q(Q^2, \omega, \eta)$ in the region $\omega \in (-1, 0)$ obeys the constraint $r_1 < 1$, whereas $r_2 < 1$ in the domain $\omega \in [0, 1)$. In order to reveal the IR renormalon structure of the Borel resummed vertex function as well as to perform numerical computations, we have to expand the hypergeometric functions over r_1 or r_2 . We choose to work in the region $\omega \in [0, 1)$, and we therefore employ the expression

$$F_{\eta' g^* g^*}^q(Q^2, \omega, \eta) = 2F_2^q(Q^2, \omega, \eta). \quad (27)$$

Due to the symmetry of $F_{\eta' g^* g^*}^q(Q^2, \omega, \eta)$ under $\omega \leftrightarrow -\omega$, the pole structure of the vertex function and numerical results in the region $\omega \in (-1, 0)$ are the same.

For the η' -meson on-shell gluon transition, we get

$$\begin{aligned} F_{\eta' gg^*}^q(Q^2, \omega = \pm 1, \eta) &= -\frac{16\pi^2 C[1+A(Q^2)]}{Q^2 \beta_0} \frac{1}{1+\eta} \int_0^\infty du e^{-ut} R(u, t) \\ &\times [B(1, 2-u) + B(2, 1-u)] + \frac{80\pi^2 C A(Q^2)}{\beta_0} \frac{1}{1+\eta} \\ &\times \int_0^\infty du e^{-ut} R(u, t) [B(3, 2-u) + B(2, 3-u)]. \end{aligned} \quad (28)$$

In the case of gluons with equal virtualities, $\omega = 0$, the $F_{\eta' g^* g^*}^q(Q^2, \omega = 0, \eta)$ can be obtained from (27) upon the substitutions $K_2 \rightarrow K_0$ and $r_2 \rightarrow r_0$, where

$$\begin{aligned} K_0(\eta) &= \frac{1}{\eta\sqrt{1+2/\eta}(1+\sqrt{1+2/\eta})}, \\ r_0 &= \frac{2}{1+\sqrt{1+2/\eta}}. \end{aligned} \quad (29)$$

As we have mentioned earlier, the massless η' -meson virtual gluon transition vertex function was computed in [22]. The predictions of this work for $F_{\eta' g^* g^*}^q(Q^2, \omega, \eta)$ should lead to the results of [22] in the limit of $\eta \rightarrow 0$. To regain these results, it is necessary to expand the relevant functions over $\eta \ll 1$, and only after that take the limit $\eta \rightarrow 0$. Then, in the general case ($\omega \neq 0, \pm 1$)

$$K_2(\omega, \eta \rightarrow 0) = \frac{1}{1+\omega}, \quad r_2 = \frac{2\omega}{1+\omega}.$$

Using the last expressions, it is not difficult to check that (27) coincides with (4.4) of [22]. By setting $\eta = 0$, from (28) one can easily recover the expression for the massless η' -meson on-shell gluon transition VF derived in (4.5) of [22].

The important question to be clarified here is whether one can use the results obtained within the RC method in the limit $Q^2 \rightarrow \infty$ in order to regain the asymptotic form of the VF. Indeed, regardless of the method used, in the limit $Q^2 \rightarrow \infty$, the VF must reach its asymptotic form, because power-suppressed corrections vanish in the asymptotic limit. In the limit $Q^2 \rightarrow \infty$, the gluon component of the η' -meson DA vanishes, $\phi^g(x, Q^2) \rightarrow 0$, whereas the quark component $\phi^q(x, Q^2)$ evolves to its asymptotic form

$$\phi^q(x, Q^2) \rightarrow 6Cx\bar{x}.$$

Therefore, the results that we obtain here not only describe the asymptotic limit of the quark component of the VF, but the asymptotic limit of the full VF itself.

From the whole analysis performed in [22] it follows that in the asymptotic limit the substitution

$$\begin{aligned} & \frac{4\pi}{\beta_0} \int_0^\infty du e^{-ut} R(u, t) B(n, m-u) \\ & \times {}_2F_1(1, m-u; m+n-u; r) \\ & \rightarrow \alpha_s(Q^2) B(n, m) {}_2F_1(1, m; m+n; r) \end{aligned}$$

has to be applied.

Having used this prescription, we obtain

$$F_{\eta' g^* g^*}^q(Q^2, \omega, \eta) \rightarrow -\frac{8\pi C \alpha_s(Q^2)}{3Q^2} K_i(\omega, \eta) {}_2F_1(1, 2; 4; r_i). \quad (30)$$

Equation (30) with the quantities labeled $i = 1, 2$, in general, should be employed in the relevant regions of the asymmetry parameter, i.e. in the regions $\omega \in (-1, 0)$ and $\omega \in (0, 1)$, respectively. But, because the hypergeometric function ${}_2F_1(1, 2; 4; z)$ is expressible in terms of the elementary ones, one can use (30) with both $i = 1$ and $i = 2$ in the whole region $\omega \in (-1, 1)$, excluding the point $\omega = 0$. At $\omega = 1$ ($\omega = -1$) (30) with $i = 2$ ($i = 1$) can be applied. Our formula for the asymptotic limit of the quark component of the VF numerically is identical to (60) of [23] (after setting there $\sqrt{n_f} f_{\eta'} \rightarrow C$ and $A_2(Q^2) = 0$ and evolving the argument of α_s to Q^2).

The IR renormalon structure of the expressions (22) and (28) does not differ from that of the corresponding massless η' -meson gluon transition FFs described in rather detailed form in [22], to which we refer interested readers.

4 The gluon component of the vertex function

We compute the gluon component of the VF, $F_{\eta' g^* g^*}^g(Q^2, \omega, \eta)$, employing the formula

$$F_{\eta' g^* g^*}^g(Q^2, \omega, \eta) = 2 \int_0^1 T_1^g(x, Q^2, \omega, \eta) \phi^g(x, Q^2) dx,$$

which leads to the following result:

$$F_{\eta' g^* g^*}^g(Q^2, \omega, \eta) = F_a^g(Q^2, \omega, \eta) + F_b^g(Q^2, \omega, \eta). \quad (31)$$

In (31) the a and b components are given by the expressions

$$\begin{aligned} & F_a^g(Q^2, \omega, \eta) \\ &= \frac{4\pi^2 CB(Q^2)}{Q^2 \beta_0 n_f} \frac{\eta}{(\omega\lambda)^2 (\omega + \eta + \omega\lambda)} \\ & \times \int_0^\infty du e^{-ut} R(u, t) \{ (1 + \omega) [B(4 - u, 2) \\ & \times {}_2F_1(1, 2; 6 - u; \bar{r}) + B(4, 2 - u) {}_2F_1(1, 2 - u; 6 - u; \bar{r})] \\ & - (1 - \omega) [B(4, 2 - u) {}_2F_1(1, 4; 6 - u; \bar{r}) \\ & + B(4 - u, 2) {}_2F_1(1, 4 - u; 6 - u; \bar{r})] \\ & - 2\omega B(3, 3 - u) [{}_2F_1(1, 3 - u; 6 - u; \bar{r}) \\ & + {}_2F_1(1, 3; 6 - u; \bar{r})] \\ & + 2\eta [B(2, 3 - u) ({}_2F_1(1, 2; 5 - u; \bar{r}) \\ & - {}_2F_1(1, 3 - u; 5 - u; \bar{r})) + B(3, 2 - u) \\ & \times ({}_2F_1(1, 2 - u; 5 - u; \bar{r}) - {}_2F_1(1, 3; 5 - u; \bar{r})) \\ & + B(4 - u, 3) ({}_2F_1(1, 3; 7 - u; \bar{r}) \\ & - {}_2F_1(1, 4 - u; 7 - u; \bar{r})) + B(4, 3 - u) \\ & \times ({}_2F_1(1, 3 - u; 7 - u; \bar{r}) - {}_2F_1(1, 4; 7 - u; \bar{r})) \} \}, \end{aligned} \quad (32)$$

where

$$\bar{r} = \frac{2\eta}{\omega + \eta + \omega\lambda}$$

and

$$\begin{aligned} & F_b^g(Q^2, \omega, \eta) \\ &= \frac{4\pi^2 CB(Q^2)}{Q^2 \beta_0 n_f} \frac{\eta}{(\omega\lambda)^2 (\eta - \omega + \omega\lambda)} \\ & \times \int_0^\infty du e^{-ut} R(u, t) \{ (1 + \omega) [B(4 - u, 2) \times \\ & \times {}_2F_1(1, 4 - u; 6 - u; r) + B(4, 2 - u) {}_2F_1(1, 4; 6 - u; r)] \\ & - (1 - \omega) [B(4, 2 - u) {}_2F_1(1, 2 - u; 6 - u; r) \\ & + B(4 - u, 2) {}_2F_1(1, 2; 6 - u; r)] \\ & - 2\omega B(3, 3 - u) [{}_2F_1(1, 3 - u; 6 - u; r) \\ & + {}_2F_1(1, 3; 6 - u; r)] + 2\eta [B(2, 3 - u) \\ & \times ({}_2F_1(1, 3 - u; 5 - u; r) - {}_2F_1(1, 2; 5 - u; r)) \\ & + B(3, 2 - u) ({}_2F_1(1, 3; 5 - u; r) \\ & - {}_2F_1(1, 2 - u; 5 - u; r)) + B(4 - u, 3) \\ & \times ({}_2F_1(1, 4 - u; 7 - u; r) - {}_2F_1(1, 3; 7 - u; r)) \\ & + B(4, 3 - u) ({}_2F_1(1, 4; 7 - u; r) \\ & - {}_2F_1(1, 3 - u; 7 - u; r)) \} \}, \end{aligned} \quad (33)$$

with $r \equiv r_2$.

It is worth noting that $F_a^g(Q^2, \omega, \eta)$ has been obtained from the original result after the transformation (26). In the region $\omega \in [0, 1)$ both r and $\bar{r} < 1$, where (32) and (33) can be used for expansion and numerical calculations. We have checked that

$$F_{\eta' g^* g^*}^g(Q^2, -\omega, \eta) = F_{\eta' g^* g^*}^g(Q^2, \omega, \eta),$$

which becomes evident if we represent the gluon component of the VF in the form

$$F_{\eta' g^* g^*}^g(Q^2, \omega, \eta) = \int_0^1 T_1^g(x, Q^2, \omega, \eta) \phi^g(x, Q^2) dx - \int_0^1 T_2^g(x, Q^2, \omega, \eta) \phi^g(x, Q^2) dx.$$

But expressions obtained using $T_2^g(x, Q^2, \omega, \eta)$ are as lengthy as the ones presented in (32) and (33); therefore, we refrain from writing them down here.

In the case of the η' -meson on-shell gluon transition, the VF can be found after changing the factors and arguments of the hypergeometric functions in (32) and (33), i.e. in $F_a^g(Q^2, \omega, \eta)$

$$\frac{\eta}{(\omega\lambda)^2(\omega+\eta+\omega\lambda)} \rightarrow \frac{\eta}{2(1+\eta)^3}, \quad \bar{r} \rightarrow \frac{\eta}{1+\eta},$$

and in $F_b^g(Q^2, \omega, \eta)$

$$\frac{\eta}{(\omega\lambda)^2(\eta-\omega+\omega\lambda)} \rightarrow \frac{1}{2(1+\eta)^2}, \quad r \rightarrow 1.$$

The gluon component of the VF is identically equal to zero for equal gluon virtualities ($\omega = 0$). This is the important qualitative modification induced by the η' -meson mass term kept in the hard-scattering amplitudes. Let us emphasize that $F_{\eta' g^* g^*}^g(Q^2, \omega = 0, \eta) \equiv 0$ within both the standard HSA and the RC method.

In the limit $\eta \rightarrow 0$ our results reproduce the expression for the gluon component of the massless η' -meson virtual gluon transition VF from (4.22) of [22]. In fact, acting as in the case of the quark component of VF, we can show that the factor in $F_a^g(Q^2, \omega, \eta)$ vanishes,

$$\frac{\eta}{(\omega\lambda)^2(\omega+\eta+\omega\lambda)} \rightarrow 0,$$

and for $F_b^g(Q^2, \omega, \eta)$ we get

$$\frac{\eta}{(\omega\lambda)^2(\eta-\omega+\omega\lambda)} \rightarrow \frac{1}{\omega(1+\omega)}, \quad r \rightarrow \frac{2\omega}{1+\omega}.$$

Then it is easy to demonstrate that the function $F_b^g(Q^2, \omega, \eta)$ in the limit $\eta \rightarrow 0$ leads to $F_{\eta' g^* g^*}^g(Q^2, \omega)$.

The infrared renormalon structure of the terms in (32) and (33) $\sim (1+\omega)$, $(1-\omega)$, 2ω are the same as in the case of the massless η' -meson virtual gluon transition VF. The terms $\sim 2\eta$ are new; nevertheless, their IR renormalon structures can be clarified using the procedures described in [22].

5 Numerical analysis

In order to start numerical computations, we need to fix the values of some constants and parameters. In our calculations the η' -meson mass is set equal to $m_{\eta'} = 0.958$ GeV. The value of the QCD scale parameter for $n_f = 4$ is $\Lambda = 0.3$ GeV.

To proceed with the computation of the η' -meson gluon vertex function and explore the role played by the η' -meson gluon content and its mass in this process, we have to define also the allowed values of the input parameters B_2^q and B_2^g at the normalization scale $\mu_0^2 = 1$ GeV 2 . In the present paper we use the η' -meson asymptotic DA or select values of the parameters B_2^q and B_2^g that obey the constraints

$$B_2^q = 0.1, \quad B_2^g \in [-2, 14]. \quad (34)$$

The quark component of the η' -meson virtual gluon transition VF for different values of the asymmetry parameter is shown in Fig. 3a. The chosen values of the input parameters correspond to the η' -meson asymptotic DA. Since, in the case of the asymptotic DA, the gluon component of the VF vanishes, in this figure we, actually, have curves for the full VF. In the same figure predictions obtained within the standard HSA are also depicted. One sees that in the domain $1 \leq Q^2 \leq 25$ GeV 2 the standard pQCD results get enhanced by approximately a factor of two due to power corrections. A similar conclusion is valid also for the gluon component of the VF for $Q^2 \geq 4$ GeV 2 (Fig. 3b) as well.

Even from these first results it is evident that soft end-point corrections lead, approximately, to the same en-

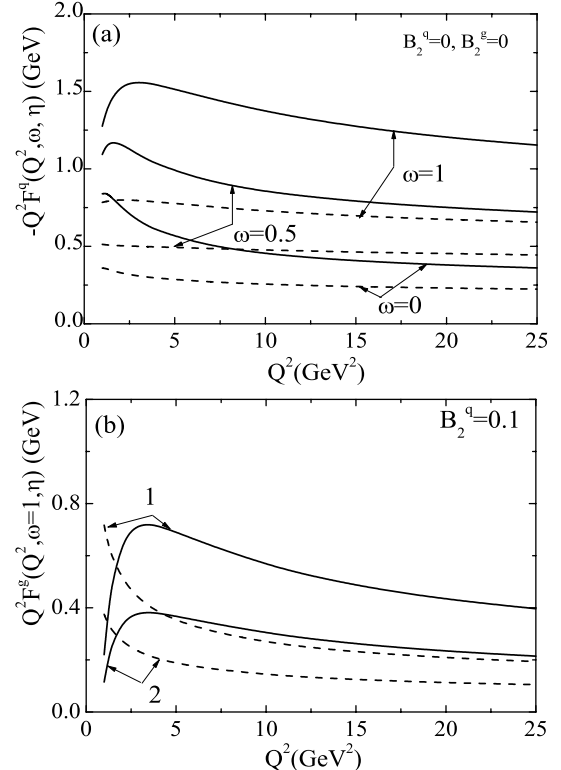


Fig. 3. The quark (a) and gluon (b) components of the scaled VF $Q^2 F_{\eta' g^* g^*}^g(Q^2, \omega, \eta)$ as functions of Q^2 . The *solid curves* are obtained using the RC method, whereas the *dashed lines* are calculated within the standard HSA. In b the correspondence between the curves and input parameter B_2^g is $B_2^g = 8$ for the curves 1 and $B_2^g = 4$ for the curves 2

hancement of the standard predictions, as in the case of the massless η' -meson virtual gluon transition [22]. Therefore, it is interesting to find modifications in the behavior of the VF induced by the η' -meson mass effects.

In Fig. 4, the VFs computed within the RC method by taking into account and neglecting the η' -meson mass term, are demonstrated. The differences in behavior of the quark component (Fig. 4a) are considerable. Indeed, mass effects suppress the absolute value of the quark component and, at the same time, change its shape in the pQCD applicable region of Q^2 . The gluon component, as a function of the total gluon virtuality Q^2 , is not affected dramatically by the η' -meson mass effects (Fig. 4b).

But the η' -meson mass term changes drastically the behavior of the gluon component of the VF as a function of the asymmetry parameter. As a function of ω , the gluon component is plotted in Fig. 5b. It turns out that $F_{\eta' g^* g^*}^g(Q^2, \omega, \eta)$ vanishes at $\omega = 0$ in the framework of both the standard HSA (the dashed lines) and the RC method (the solid lines). For small ω the end-point effects are also mild. Therefore, it is legitimate to conclude that in the region $|\omega| < 0.2$, $F_{\eta' g^* g^*}^g(Q^2, \omega, \eta)$ feels neither end-point nor mass effects. The dependence of the quark component $F_{\eta' g^* g^*}^q(Q^2, \omega, \eta)$ on ω is plotted in panel (a) of the same fig-

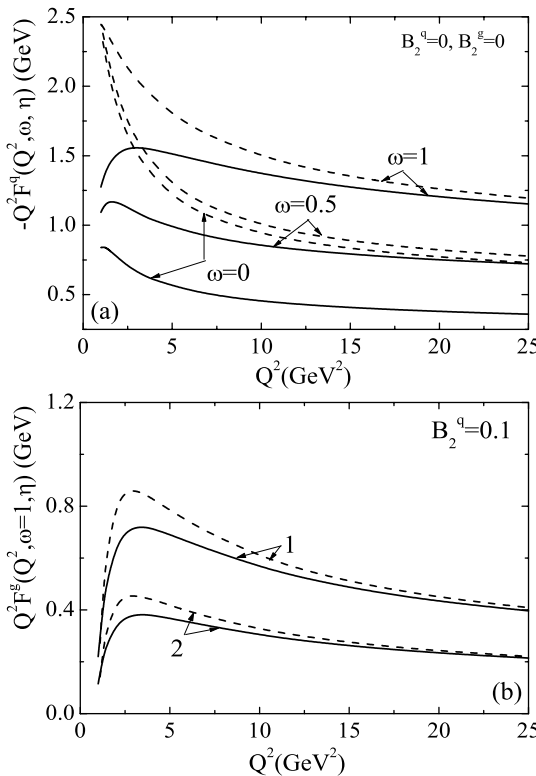


Fig. 4. The quark (a) and gluon (b) components of the VF versus Q^2 . All curves are obtained in the context of the RC method. The *solid lines* are calculated by taking into account the η' -meson mass effects: in computations of the *dashed lines* the η' -meson mass term is neglected. In b the correspondence between the curves and parameter B_2^g is the same as in Fig. 3

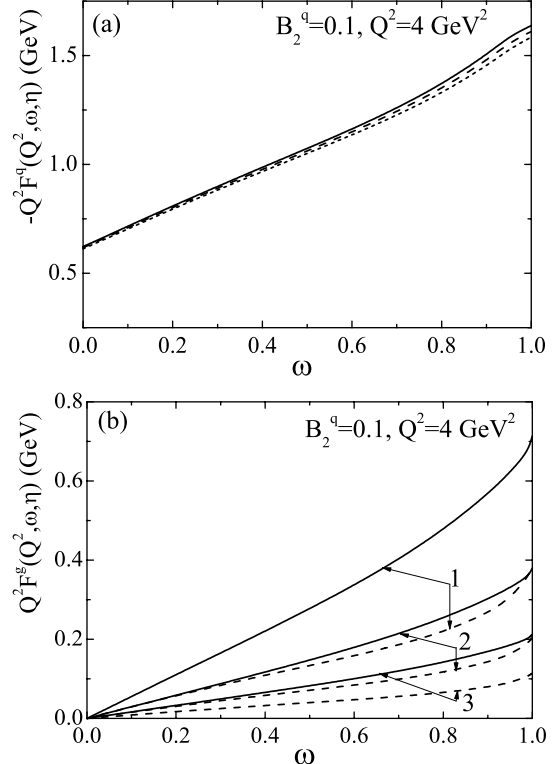


Fig. 5. The quark (a) and gluon (b) components of the VF at fixed B_2^q and Q^2 versus ω . In a all curves are obtained in the context of the RC method. The correspondence between them and the parameter B_2^g is: $B_2^g = 0$ for the *solid curve*; $B_2^g = 4$ for the *dashed curve*; $B_2^g = 8$ for the *short-dashed curve*. In b the *solid curves* are obtained within the RC method. For computation of the *broken lines* the standard HSA is used. The correspondence between the curves and the parameter B_2^g is $B_2^g = 8$ for the curves 1; $B_2^g = 4$ for the curves 2 and $B_2^g = 2$ for the lines 3

ure: as a function of ω it demonstrates firm stability against variations of B_2^g .

We have analyzed the impact of the various DAs of the η' -meson on the VF. The quark component of the VF is stable for different values of $B_2^g \in [0, 8]$ (Fig. 6, panel (a)). In contrast, the gluon component of the VF demonstrates rapid growth with B_2^g (Fig. 6b). As a result, due to different signs of the quark and gluon components of the VF, the total vertex function $F_{\eta' gg^*}(Q^2, \omega = \pm 1, \eta)$ for $B_2^g \neq 0$ runs below the asymptotic one (Fig. 7a). For comparison the predictions derived in the standard HSA are also shown (Fig. 7b). The quantitative difference between the corresponding curves is clear.

The dependence of the full VF on the asymmetry parameter ω is depicted in Fig. 8. In the calculations the η' -meson DAs with various values of B_2^g are employed. As has been noted above, the gluon component of the VF is identically equal to zero at $\omega = 0$, and the quark component, as a function of ω , demonstrates stability against variations of B_2^g . Therefore, it is easy to understand the features of the full VF as a function of ω . Really, in the region $|\omega| < 0.3$ the difference between the VFs corresponding to different B_2^g is small; it becomes essential for $|\omega| > 0.8$. But, owing

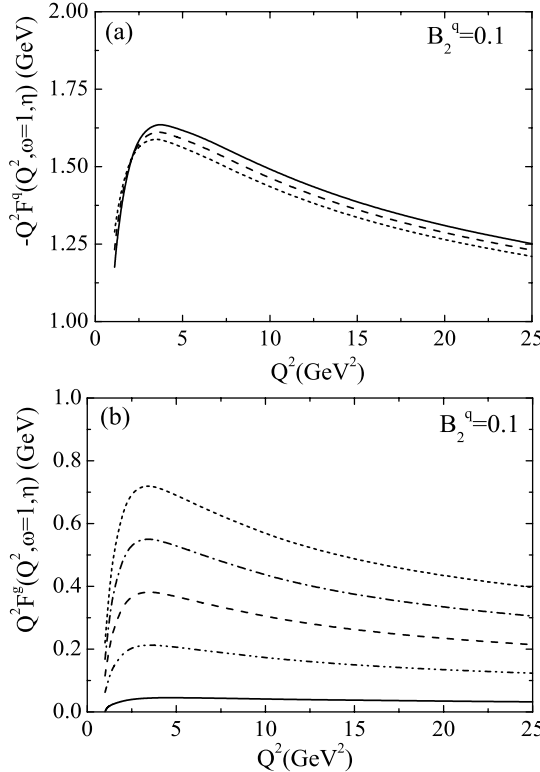


Fig. 6. The quark (a) and gluon (b) components of the VF as functions of Q^2 at $\omega = \pm 1$. All curves are computed using the RC method. The correspondence between plotted curves and parameter B_2^q is $B_2^q = 0$ for the solid curves; $B_2^q = 2$ for the dot-dot-dashed curves; $B_2^q = 4$ for the dashed lines; $B_2^q = 6$ for the dot-dashed lines and $B_2^q = 8$ for the short-dashed curves

to the power corrections, mainly to the quark component, even for $|\omega| < 0.3$ the Borel resummed full VF significantly exceeds the standard pQCD result.

For phenomenological applications it is useful to parameterize the VF using some simple expressions. We start from the expressions of the VF obtained in the framework of the standard HSA. For the sake of simplicity, let us consider the η' -meson asymptotic DA. In this case, the standard pQCD prediction for the VF is given by (30). Now, we want to approximate the RC prediction in the form

$$F_{\eta' g^* g^*}^q(Q^2, \omega, \eta) = -\frac{8\pi C \alpha_s(Q^2)}{3Q^2} K_2(\omega, \eta) \times {}_2 F_1(1, 2; 4; r_2) \left(a + \frac{b}{Q^2} + \frac{c}{Q^4} + \dots \right). \quad (35)$$

From the general formula (35), for the η' -meson on-shell gluon transition we get

$$F_{\eta' gg^*}^q(Q^2, \omega = \pm 1, \eta) = -\frac{4\pi C \alpha_s(Q^2)}{Q^2} \times \frac{1}{1 + \eta} \left(a + \frac{b}{Q^2} + \frac{c}{Q^4} + \dots \right). \quad (36)$$

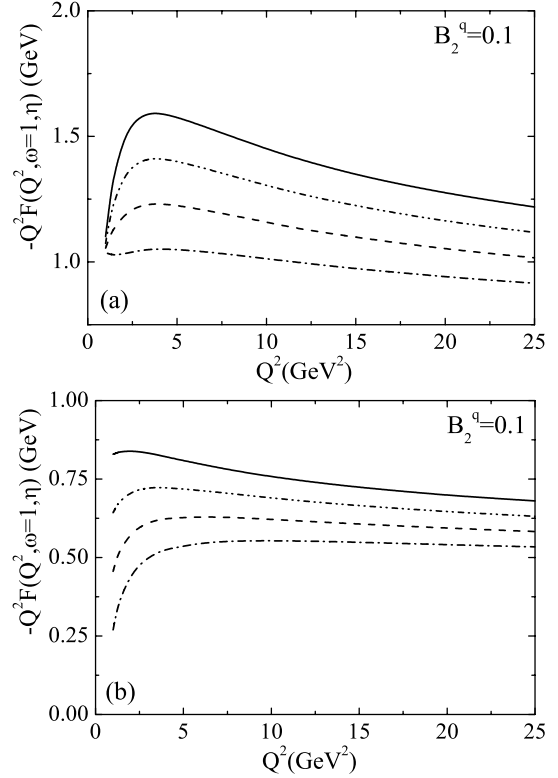


Fig. 7. The full VF at $\omega = \pm 1$ computed using the RC method (a) and the standard HSA (b). The correspondence between the depicted lines and the parameter B_2^g is the same as in Fig. 6 (the short-dashed lines are not shown)

The fitting procedure gives the following values of the parameters:

$$a \simeq 1.7837, \quad b \simeq 0.8228, \quad c \simeq -1.022.$$

In the case of the gluons with equal virtualities, we find

$$F_{\eta' g^* g^*}^q(Q^2, \omega = 0, \eta) = -\frac{8\pi C \alpha_s(Q^2)}{3Q^2} K_0(\eta) {}_2 F_1(1, 2; 4; r_0) \times \left(a + \frac{b}{Q^2} + \frac{c}{Q^4} + \dots \right), \quad (37)$$

with

$$a \simeq 1.5485, \quad b \simeq 2.3361, \quad c \simeq -1.627.$$

The corresponding results are shown in Fig. 9. As is seen, (37) leads to an almost perfect approximation of the original result, whereas the expression (36) describes the exact prediction, demonstrating, nevertheless, some deviations.

It is known that the RC method produces higher-twist ambiguities. For the massless η' -meson gluon transition VF they were estimated in [22] and found to lie within $\pm 15\%$ of the original results. Because such modifications cannot change our principal conclusions, we do not concentrate on these questions here.

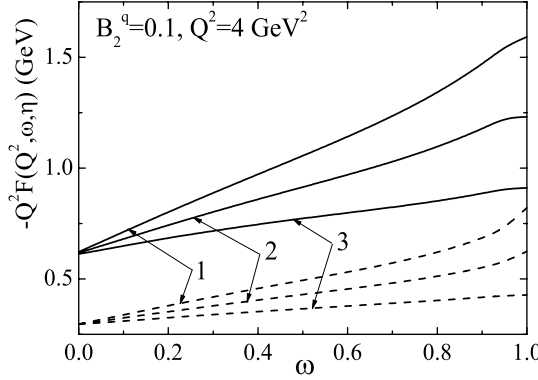


Fig. 8. The full VF obtained by employing the RC method (the *solid lines*) and the standard HSA (the *dashed lines*) as a function of ω . For the lines 1 the parameter is $B_2^g = 0$; for the lines 2 $B_2^g = 4$, and for the lines 3 $B_2^g = 8$

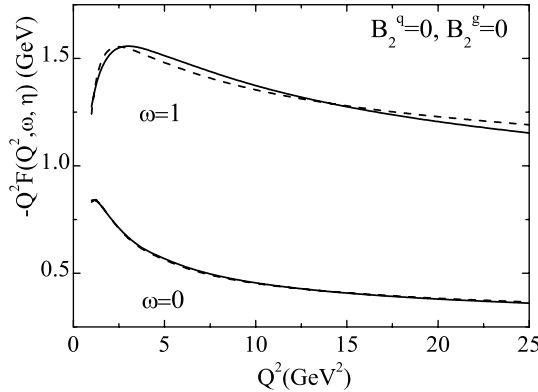


Fig. 9. The approximations to the full VF. For the *upper curves* $\omega = 1$, for the *lower ones* $\omega = 0$. The *solid lines* are RC predictions, the *dashed ones* the corresponding approximations

6 Concluding remarks

In this paper we have evaluated soft end-point (power-suppressed) corrections to the space-like η' -meson virtual gluon transition VF by including the η' -meson mass effects. To this end, we have employed the standard HSA and RC method in conjunction with the IR renormalon calculus. In the calculations, both the quark and the gluon components of the η' -meson DA have been taken into account. We have modelled the DAs by retaining in the general expressions (6) and (7) only the first non-asymptotic terms.

We have extended the results obtained in [22] for the massless η' -meson virtual gluon transition VF. It has been shown that effects generated by the η' -meson mass term considerably change the predictions obtained in [22]: they suppress the absolute values of the quark and gluon components of the VF, and modify their behavior as functions of the asymmetry parameter ω . This modification, in the case of the gluon component, has not only a quantitative, but also a qualitative character: thus, at $\omega = 0$ the gluon component of the VF vanishes identically. As a result, mass effects change the dependence of the full VF on the total gluon virtuality Q^2 and asymmetry parameter ω .

The numerical analysis presented shows that power corrections considerably enhance the standard pQCD predictions for the VF in the explored region $1 \text{ GeV}^2 \leq Q^2 \leq 25 \text{ GeV}^2$, though other sources may also give rise to power corrections. As an important consistency check, we have proven that the results obtained within the RC method in the asymptotic limit $Q^2 \rightarrow \infty$ reproduce the standard pQCD predictions for the vertex function.

References

1. CLEO Collaboration, J. Gronberg et al., Phys. Rev. D **57**, 33 (1998) [hep-ex/9707031]
2. CLEO Collaboration, B.H. Behrens et al., Phys. Rev. Lett. **80**, 3710 (1998) [hep-ex/9801012]
3. T.E. Browder et al., Phys. Rev. Lett. **81**, 1786 (1998) [hep-ex/9804018]
4. T. Feldmann, P. Kroll, Eur. Phys. J. C **5**, 327 (1998) [hep-ph/9711231]
5. J. Cao, F.-G. Cao, T. Huang, B.-Q. Ma, Phys. Rev. D **58**, 113006 (1998) [hep-ph/9807508]
6. S.S. Agaev, Phys. Rev. D **64**, 014007 (2001)
7. S.S. Agaev, N.G. Stefanis, Phys. Rev. D **70**, 054020 (2004) [hep-ph/0307087]
8. P. Kroll, K. Passek-Kumericki, Phys. Rev. D **67**, 054017 (2003) [hep-ph/0210045]
9. A. Ali, A.Y. Parkhomenko, Eur. Phys. J. C **30**, 183 (2003) [hep-ph/0304278]
10. D. Atwood, A. Soni, Phys. Lett. B **405**, 150 (1997) [hep-ph/9704357]
11. W.-S. Hou, B. Tseng, Phys. Rev. Lett. **80**, 434 (1998) [hep-ph/9705304]
12. A.L. Kagan, A.A. Petrov, hep-ph/9707354
13. M. Ahmady, E. Kou, A. Sugamoto, Phys. Rev. D **58**, 014015 (1998) [hep-ph/9710509]
14. A. Ali, J. Chay, C. Greub, P. Ko, Phys. Lett. B **424**, 161 (1998) [hep-ph/9712372]
15. D. Du, C.S. Kim, Y. Yang, Phys. Lett. B **426**, 133 (1998) [hep-ph/9711428]
16. Y.Y. Keum, H.-N. Li, A.I. Sanda, Phys. Rev. D **63**, 054008 (2001) [hep-ph/0004173]
17. Y.Y. Keum, H.-N. Li, Phys. Rev. D **63**, 074006 (2001) [hep-ph/0006001]
18. Y.-Y. Charng, T. Kurimoto, H.-N. Li, Phys. Rev. D **74**, 074024 (2006) [hep-ph/0609165]
19. J.O. Eeg, A. Hiorth, A.D. Polosa, Phys. Rev. D **65**, 054030 (2002) [hep-ph/0109201]
20. J.O. Eeg, K. Kumericki, I. Picek, Phys. Lett. B **563**, 87 (2003) [hep-ph/0407279]
21. T. Muta, M.-Z. Yang, Phys. Rev. D **61**, 054007 (2000) [hep-ph/9909484]
22. S.S. Agaev, N.G. Stefanis, Eur. Phys. J. C **32**, 507 (2004) [hep-ph/0212318]
23. A. Ali, A.Y. Parkhomenko, Eur. Phys. J. C **30**, 367 (2003) [hep-ph/0307092]
24. S.S. Agaev, Phys. Lett. B **360**, 117 (1995) [Erratum Phys. Lett. B **369**, 379 (1996)]
25. S.S. Agaev, ICTP preprint IC/95/291, hep-ph/9611215
26. G.P. Lepage, S.J. Brodsky, Phys. Rev. D **22**, 2157 (1980)

- 27. A.V. Efremov, A.V. Radyushkin, Phys. Lett. B **94**, 245 (1980)
- 28. A. Duncan, A.H. Mueller, Phys. Rev. D **21**, 1636 (1980)
- 29. M. Beneke, Phys. Rep. **317**, 1 (1999) [hep-ph/9807443]
- 30. A. Grozin, hep-ph/0311050
- 31. S.S. Agaev, Eur. Phys. J. C **1**, 321 (1998) [hep-ph/9611283]
- 32. S.S. Agaev, Phys. Rev. D **69**, 094010 (2004) [hep-ph/0403161]
- 33. S.S. Agaev, M. Guidal, B. Pire, Eur. Phys. J. C **37**, 457 (2004) [hep-ph/0403266]
- 34. M. Franz, P.V. Pobylitsa, M.V. Polyakov, K. Goeke, Phys. Lett. B **454**, 335 (1999) [hep-ph/9810343]
- 35. M. Franz, M.V. Polyakov, K. Goeke, Phys. Rev. D **62**, 074024 (2000) [hep-ph/0002240]
- 36. A. Petrov, Phys. Rev. D **58**, 054004 (1998) [hep-ph/972497]
- 37. T. Feldmann, Int. J. Mod. Phys. A **15**, 159 (2000) [hep-ph/9907491]